Gene variants in *ZGRF1* implicated for a rare sensory reflex epilepsy

Shalini Roy Choudhury [1], Parthasarathy Satishchandra [3], Sanjib Sinha [3], Anuranjan Anand [1,2]

[1] Molecular Biology and Genetics Unit, Jawaharlal Nehru Centre for Advanced Scientific Research (JNCASR), Bangalore 560 064, India

[2] Neuroscience Unit, Jawaharlal Nehru Centre for Advanced Scientific Research, Bangalore 560 064, India

[3] Department of Neurology, National Institute of Mental Health and Neurosciences (NIMHANS), Bangalore 560 029, India

Correspondence

Anuranjan Anand, Molecular Biology and Genetics Unit, Neuroscience Unit, Jawaharlal Nehru Centre for Advanced Scientific Research, Jakkur, Bangalore 560064, Karnataka, India. Email: anand@jncasr.ac.in

Abstract: Hot water epilepsy (HWE) is a rare sensory reflex epilepsy syndrome where seizures are precipitated by a stimulus of contact with hot water. While there is genetic basis to its etiology, identity of specific genes underlying this relatively uncommon disorder has remained unknown. Here, we present our studies aimed at identifying a causative gene in a four-generation family (Family 227) with several of its members affected with the disorder, from the southern parts of India. We conducted whole exome-based sequencing, and examined the HWE genetic locus previously known to map to 4q24-q28 (*HWE2*, MIM: 613340) in the family and identified a sequence variant, c.1805C>T (p.Thr602Ile) in *ZGRF1* co-segregating with the disorder. Complete transcript structure of *ZGRF1* was examined in 288 HWE patients and five missense variants, Arg326Gln, Glu660Gly, Arg1862*, Phe1940Leu and Asp1984Gly, present exclusively or almost exclusively in the patients were found. Functional correlates of the six variants identified were examined in cultured mammalian cells. We observed spindle pole defects during cell division and partially disrupted localization of UPF1, a protein involved in cell cycle regulation, at spindles. Our observations provide insights into the genetic basis of HWE and suggest involvement of unanticipated molecular mechanisms underlying this neurobehavioral phenotype.

Introduction

Sensory reflex epilepsy comprises a class of rare human epilepsies (Italiano et al., 2016) where seizures are triggered by a wide range of sensory stimuli. A somatosensory stimulus of contact with hot water at temperature ranging between 40-50˚C, has been known to trigger the onset of seizures in a condition known as hot water epilepsy (HWE). It is also known as water immersion epilepsy or bathing epilepsy. HWE was first reported from New Zealand (Allen, 1945), following which there have been reports from different parts of the world: Australia (Keipert, 1969), the United States (Stensman and Ursing, 1971), India (Mani et al., 1974; Satishchandra et al., 1988; Satishchandra, 2003), the United Kingdom (Moran, 1976), Canada (Szymonowicz and Meloff, 1978), Japan (Kurata, 1979; Morimoto et al., 1985) and Turkey (Bebek et al., 2001). Majority of the HWE cases have been reported from India. HWE is prevalent in the southern parts of the country where hot water bathing after applying hot oil on the head is a cultural custom. The seizures are often manifested with symptoms that include dazed look, state of confusion, indistinct speech, epigastric sensations and compulsive behavior (Satishchandra, 2003). Individuals with HWE exhibit psychiatric symptoms during the phase of aura, with a sense of fear, visual and auditory hallucinations, déjà vu, and experience feelings of living in the future. About 10% of the patients are habituated to self-induction of seizures with a sense of intense desire and pleasure, provoking these patients to continuously pour hot water over their head to induce seizures (Satishchandra et al., 1988). Both the temperature of water and the contact sensation seem to be important aspects in the phenotypic manifestation of this disorder.

While the first case of HWE was reported as early as 1945 (Allen, 1945), genetic basis of this disorder are only now beginning to be examined. Familial clustering and positive family histories have been reported for 7-15% of the patients from India (Mani et al 1974, Satishchandra et al 1988) and for 10% of the patients from Turkey (Bebek et al., 2001). Three HWE loci are known to map to 10q21.3-q22.3 (*HWE1*, MIM: 613339; Ratnapriya et al., 2009a), 4q24-q28 (*HWE2*, MIM: 613340; Ratnapriya et al., 2009b) and 9p24.3-p23 (Karan et al., 2018). Mutations in *SYN1* have been reported in a French-Canadian family with X-linked focal epilepsy and reflex bathing seizures (Nguyen et al., 2015). A loss of function mutation in *GPR56* has been identified in a 5-year old Portuguese boy with bilateral frontoparietal polymicrogyria who presented with HWE (Santos-Silva et al., 2015). Partial loss-of-function at *SLC1A1* has been reported in HWE families from India (Karan et al., 2017). We examined the 4q24-q28 (*HWE2*) locus to identify the causative gene for epilepsy

in Family 227. Here, we report our studies indicating the involvement of the *ZGRF1* (zinc finger GRF-type containing 1) gene variants in HWE.

Subjects and methods

Family ascertainment and clinical characterization

Hot water epilepsy families were ascertained at the Department of Neurology, National Institute of Mental Health and Neurosciences (NIMHANS), Bangalore. Family 227 is a four-generation family of 28 members, of which 10 were affected, 3 clinically asymptomatic and 15 unaffected (Figure 1A). HWE in the family is transmitted in an apparently autosomal dominant mode with incomplete penetrance. Clinical diagnoses were made by qualified neurologist according to ILAE guidelines for epilepsy classification (ILAE 2001) and clinical criterion for seizures upon hot water bath based on clinical histories. Information regarding seizures and family histories of epilepsy or other neurological disorders, required for diagnosis was obtained from patients and family members who had witnessed such episodes in the affected individuals. Family 227 was recruited through the proband III:7, diagnosed with HWE at 20 years of age. His seizure episodes were characterized by the features of HWE and his inter-ictal EEG showed discharges arising in the left anterior temporal region. No hippocampal abnormality was detected. He was treated with intermittent prophylactic clobazam therapy. Two individuals, II:7 and IV:1 had histories of febrile convulsions (FCs). Three individuals II:2, II:3 and III:2 were asymptomatic but had at least one child manifesting HWE. Peripheral blood samples were collected from each participating individual and DNA was isolated from the white blood cells using a standard phenol-chloroform method. This study had approval of the Institutional Human Bioethics Committees of the NIMHANS and JNCASR. All individuals in the family who participated in this study provided informed written consent.

DNA sequencing and analysis

Whole exome sequencing was carried out for an affected parent-offspring pair, III:4 and IV:3, using the Agilent SureSelect Human All Exon 50 Mb Kit (Agilent Technologies, Santa Clara, USA). Genomic DNA sequencing libraries were prepared according to manufacturer's protocol (Agilent). Briefly, genomic DNA was fragmented, purified, analyzed for size distribution and concentration, and adapters were ligated. The libraries were sequenced for 100 bp paired-end reads on Illumina Genome Analyzer (GAIIx). Reads with at least 70% of

the bases having a minimum Phred score of 20 were obtained by SeqQC-V2.0. FASTQ files were trimmed and aligned to the reference human genome (hg19, GRCh37) using Burrows-Wheeler Aligner (BWA)-0.6.0 (Li and Durbin, 2009). Duplicate reads and those with inappropriate read pair were removed using SAMtools v0.1.7a (Li et al., 2009). Alignment statistics were obtained from BEDTools v-2.12.0 (Quinlan and Hall, 2010). Variants were called by SAMtools at a Phred like SNP quality score of ≥20 and annotated against dbSNP131 and dbSNP135. Sequence reads at the locus were manually examined and updated control frequencies of annotated variants were confirmed in the dbSNP144, 1000 Genomes, Exome Variant Server (ESP), and The Genome Aggregation Database (gnomAD). About 8% of the 4q24-q28 locus not covered by exome sequencing was Sanger sequenced using specific primer pairs. Common variants with a minor allele frequency (MAF)>0.005 across databases within the target region 4q24-q28 (between D4S1572 and D4S2277) were excluded from further analysis. Variants with MAF ≤ 0.005, present in the exons, flanking introns (±100bp) and UTRs were examined further. Rare, heterozygous variants were confirmed by Sanger sequencing, examined for segregation in the family and coded according to HGVS (Human Genome Variation Society).

Mutation analysis of *ZGRF1* in HWE patients

The complete transcript structure of *ZGRF1* (RefSeq NM_018392.4) comprising 27 coding exons, flanking introns, 5'UTR and 3'UTR was amplified in 288 HWE patients and ethnicity-matched controls using an ABI9700 Thermal Cycler (Applied Biosystems, Foster City, USA). The amplified products were sequenced using BigDye^{TM} Terminator Cycle Sequencing v3.0 reagents (Applied Biosystems) and were analysed on an ABI3730 Genetic Analyzer (Applied Biosystems).

Mutagenesis

The full-length cDNA of *ZGRF1* cloned into mammalian pCMV6 vector with C-terminal Myc-DDK tag (RC229463, Origene) was used as the template for introducing six *ZGRF1* variants: Arg326Gln-, Thr602Ile-, Glu660Gly-, Arg1862*-, Phe1940Leu- and Asp1984Gly. Mutagenesis was performed using the QuikChange II XL Site-Directed Mutagenesis kit (Agilent). Plasmids with the *ZGRF1* variants were purified using QIAprep Spin Miniprep columns (Qiagen, Hilden, Germany) and confirmed by Sanger sequencing. (For a complete list of the primers used for ZGRF1 sequencing, see Supplementary Tables S1, S2 and S3).

Reverse-transcription polymerase chain reaction

Brain cDNA from cerebral cortex, cerebellum, hippocampus and hypothalamus (Takara Bio, Santa Clara, USA) was used to examine the expression of *ZGRF1* transcripts in the human brain. Two primer pairs 5'-TCCAAAGACACAGAAGCACA-3' and 5'-ACCTGC AAGAAGTCAATCTGC-3', and 5'-TCAGCCTAGGAGCAACATTGA-3' and 5'-TCCAA CTACTCGAACCTGCT-3' were used to amplify cDNA from the N-terminal and C-terminal regions of *ZGRF1*, respectively. The amplified products were purified using Qiaquick columns (Qiagen) and sequence confirmed.

Cell culture and transfection

HEK293 (ATCC, Manassas, USA), SH-SY5Y (ATCC) and C6 glioma (ECACC, Sigma-Aldrich, St. Louis, USA) cells were cultured in DMEM supplemented with 10% heat-inactivated fetal bovine serum for up to 10 passages. For protein overexpression studies in HEK293 cells, transfection was carried out with 4.5 µg of plasmid using the calcium phosphate method. Cells were seeded in 35 mm dishes (for protein immunoblot analysis) or in poly-L-lysine coated coverslips (for immunocytochemistry assays). Cells were seeded 24 h before transfection, and experiments were performed 48 h after transfection.

Immunocytochemistry

Cells were washed with PBS, fixed with 2% paraformaldehyde or methanol for 15 min, permeabilized with 0.1% Triton X-100 for 10 min, incubated with blocking solution (5% BSA in PBS) for 4 h at 4°C, and stained overnight at 4°C with primary antibodies. Primary antibodies used in these experiments were: (1) rabbit polyclonal anti-ZGRF1 (1:100 for endogenous expressions, 1:1000 for overexpression studies; ab122126, Abcam, UK) (2) mouse monoclonal anti-γ-tubulin (1:5000, T5326, Sigma-Aldrich) and (3) rabbit monoclonal anti-UPF1 Alexa Fluor 488 (1:100, ab201761, Abcam). The cells were washed with PBS and incubated with secondary antibodies conjugated with Alexa Fluor-568 or Alexa Fluor-488 (Invitrogen Molecular probes, Waltham, USA) for 4 h at 4°C. Cells were then washed with PBS and counterstained with DAPI (Sigma-Aldrich). For synchronization experiments, HEK293 cells were incubated in culture medium containing 2 mM thymidine (Sigma-Aldrich) for 14 h, followed by mitotic enrichment in medium containing 24 µM deoxycytidine (Sigma-Aldrich) for 9 h. Three hundred transfected, mitotic cells were counted for the wild-type and six variant alleles of *ZGRF1*. Coverslips were mounted in 70% glycerol (Merck Millipore, Burlington, USA) and imaged on an LSM 880 Meta confocal

laser scanning microscope (Carl Zeiss, Oberkochen, Germany) under a 63x/1.4 oil immersion objective. Images were processed and scale bars were added in Zen (Carl Zeiss). All statistical comparisons were done using GraphPad Prism5. One-way ANOVA followed by Dunnett‘s test for multiple comparisons were used for statistical analysis between the wild-type and variants. Results are shown as mean ± standard error of the mean (SEM). Differences between groups were considered statistically significant for $P \leq 0.05$ and $P \leq 0.001$.

Immunoblot analysis

Cells were lysed in 200µl of RIPA lysis buffer (50 mM Tris-HCl pH 7.4, 150 mM NaCl, 1 mM EDTA, 0.5% sodium deoxycholate, 1% NP-40 and 0.1% SDS) supplemented with protease inhibitor cocktail (Sigma-Aldrich) for 3 h at 4°C in a rotating mixer. Lysed cells were spun down at 14,000 g for 20 min at 4°C and protein concentration was determined using the bicinchoninic acid assay (Sigma-Aldrich). Approximately 50 µg of protein was loaded on an 8% polyacrylamide gel along with pre-stained protein ladder (Bio-Rad Laboratories, Hercules, USA). Proteins from the gel were electro-transferred to 0.45µm PVDF membrane (Millipore) using a wet electroblotting system (Bio-Rad) at a constant voltage of 100 V for 1 h in the transfer buffer (25 mM Tris-HCl, 192 mM glycine, 20% methanol and 0.036% SDS) at 4°C. The membrane was blocked in 5% skimmed milk (HiMedia, Mumbai, India) for 4 h at 4°C, incubated overnight at 4°C in primary antibodies rabbit polyclonal anti-ZGRF1 (1:300, ab122126) or γ-tubulin (1:5000, T5326). The blot was washed in PBS, incubated for 1 h at room temperature with rabbit or mouse horseradish peroxidase (HRP)-conjugated secondary antibodies (1:5000, Bangalore GeNei, Bangalore, India) and washed with PBS containing 0.1% Tween-20. Protein bands were detected using an enhanced chemiluminiscent substrate for HRP (West Pico, Pierce, Waltham, USA). Lysates (50µg) from different regions of the brain: amygdala, basal ganglia, cerebellum, hippocampus and hypothalamus were loaded on a 5-15% gradient gel, transferred on to a 0.45µm nitrocellulose membrane (GE Healthcare Life Sciences, Marlborough, USA) using a semi-dry transfer system (Bio-Rad Laboratories), and the membrane was processed as above.

Bioinformatic analysis

The complete nucleotide sequence of *ZGRF1* is available at NCBI (Accession Number NC_000004.11, assembly GRCh37, annotation release 105). It comprises 97.66 kb of

sequence length spanning 113,460,489-113,558,151 bases (GRCh37 co-ordinates). Primers used in this study were designed using Primer3. Nucleotide and protein sequences across different species were obtained from NCBI HomoloGene database. Sequence conservation and multiple sequence alignment analyses were carried out by Clustal Omega. Potential pathogenic effects of the variants were predicted using SIFT (Kumar et al., 2009), PolyPhen-2 (Adzhubei et al., 2010), Mutation Taster (Schwarz et al., 2010), and FATHMM (Shihab et al., 2013). pBLAST (protein-protein BLAST) was used to determine ZGRF1 homologs and DELTA-BLAST (Domain Enhanced Lookup Time Accelerated BLAST; Boratyn et al., 2012) was used to predict the domain architecture of ZGRF1. Domain-wise identities and similarities were determined by pairwise alignment using EMBOSS Needle.

Results

Rare variant prioritization

We performed whole exome sequencing on two affected individuals III:4 and IV:3 from the family. For both the individuals, we obtained a mapping efficiency of 95.7%, and 92% coverage of the exonic regions with ≥10 reads, at the 4q24-q28 locus (Supplementary Tables S4 and S5). Employing a combination of exome-based and Sanger-based sequencing, we identified 573 variants at the target region, among the two individuals (Figure 1B). Among these, 544 were relatively common variants (MAF > 0.005) across the different control databases. The remaining 29 rare variants (MAF ≤ 0.005, Supplementary Tables S6 and S7) were confirmed for their presence/absence and zygosity in the two exome sequenced family members. Nineteen among the 29 variants were either homozygous, or heterozygous and present in one of the affected members. These variants were not considered further. The remaining ten variants were heterozygous and present in both III:4 and IV:3, and were examined for segregation in the family. Nine among these ten variants did not segregate. We found one non-synonymous, heterozygous variant, c.1805C>T located in exon 5 of the *ZGRF1* (zinc finger GRF-type containing 1) gene to co-segregate with the disorder in the family. *ZGRF1*, c.1805C>T leads to an amino acid change, p.Thr602Ile in the ZGRF1 protein (Figure 1C). Among the available ZGRF1 protein sequences, this residue is conserved among higher mammals, namely, *H. sapiens*, *M. mulatta*, *B. taurus* and *P. troglodytes*.

ZGRF1 encodes a transcript of 6652 bases and a protein of 2104 amino acids. According to HGNC (HUGO Gene Nomenclature Committee), ZGRF1 belongs to the family of zinc-finger GRF-type and UPF1-like RNA helicases. There are at least six additional GRF-type proteins, and 11 proteins that belong to the UPF1-like RNA helicases family. These are spliceosomal factors, DNA/RNA helicases or nucleases. *In-silico* analyses of the ZGRF1 sequence identified three main domains in the protein (Supplementary Figure S8a). An N-terminal *first domain* DUF2439 (domain of unknown function 2439) encompasses 70 amino acids. Orthologs of this domain are found in *Schizosaccharomyces pombe, Saccharomyces cerevisiae* and *Arabidopsis thaliana* (Polakova et al., 2016). This domain has been implicated in meiotic chromosome segregation, crossover recombination and telomere maintenance (Polakova et al., 2016; Silva et al., 2016). A centrally placed *second domain* zf-GRF (zinc finger-GRF type) is a presumed zinc binding domain of 45 amino acids named after three conserved residues within the domain. This domain is present in proteins with helicase, nuclease, polymerase or topoisomerase activities. The C-terminus has the *third domain* comprising four approximately overlapping domains with predicted helicase activities, which we collectively refer to as the helicase domain. These are the AAA_11, AAA_12/UvrDC2, DNA2 and recD domains. AAA_11 and AAA_12/UvrDC2 spans 231 and 185 amino acids, respectively. They belong to a large and functionally diverse AAA superfamily (ATPase Associated with diverse cellular Activities) of ring-shaped P-loop NTPases that function as molecular chaperons (Iyer et al., 2004) through energy-dependent unfolding of macromolecules (Frickey and Lupas, 2004). The DNA2 domain of 319 amino acids belong to the superfamily I (SF1) DNA and/or RNA helicase. Structural data is available for a single SF1 RNA helicase, UPF1 (up-frameshift 1), a protein involved in nonsense-mediated mRNA decay (Cheng et al., 2007). Biochemical analysis of SF1 RNA helicases have revealed dual RNA- and DNA- stimulated ATPase and helicase activities (Raney et al., 2013). The recD domain spanning 44 amino acids are DNA helicases.

ZGRF1 variants in additional HWE patients

We examined the complete transcript structure of *ZGRF1* among 288 HWE patients. In this analysis (Table 1), we identified six rare missense variants in the gene: c.977G>A (p.Arg326Gln), c.1805C>T (p.Thr602Ile) and c.1979A>G (p.Glu660Gly) located in the long non-domain region towards the N-terminus of the protein placed between the DUF2439 and zf-GRF domains; and, three variants c.5584C>T (p.Arg1862*), c.5818T>C (p.Phe1940Leu) and c.5951A>G (p.Asp1984Gly) within the helicase domain, towards the C-terminus (Figure

1C, Supplementary Figure S8b). These six non-synonymous variants were either absent or rare among 576 population-matched control chromosomes of individuals from the southern parts of India, as well as among the four variant databases: dbSNP, 1000 Genomes, ESP and gnomAD. The amino acid residues Arg1862 and Phe1940 are well conserved across different species examined, Glu660 and Asp1984 are conserved among all species except *G.gallus* and Arg326 is conserved among all species and absent in *G.gallus* (Figure 1D). We also found 29 single nucleotide polymorphisms in the *ZGRF1* gene that were common among population-matched controls and in databases (Supplementary Table S9).

ZGRF1 expression in the human brain

ZGRF1 is expressed in the human brain regions. We amplified ZGRF1 transcripts from Marathon-Ready™ full-length brain cDNAs from human cerebral cortex, cerebellum, hippocampus, and hypothalamus. The bands (Figure 2A) corresponded to the expected sizes of 656 bases and 572 bases for the N-terminal ad C-terminal regions, respectively. We gel extracted the bands and confirmed them by sequencing. Western blot analysis indicated immunoreactivity to the anti-ZGRF1 antibody in amygdala, basal ganglia, cerebellum, hippocampus and hypothalamus of the human brain (Figure 2B). The *ZGRF1* transcripts are reported to be ubiquitously present across different human tissues (Human Protein Atlas RNA-sequencing data).

ZGRF1 expression during mitotic stages

In cultured HEK293 cells, ZGRF1 showed localization in the cell cytoplasm. We observed that, the protein has distinct localization pattern in mitotic cells. ZGRF1 localizes at the centrosomes during prophase and at the spindle poles during metaphase and anaphase stages (Figure 2C). The protein localized to midbodies during telophase and cytokinesis stages. Some cells also expressed the protein in the nucleolus. In SH-SY5Y neuroblastoma and rat C6 glioma cells, the protein localized in a similar manner, in the cytoplasm and could be detected at the spindles poles in dividing cells (Figure 2D). ZGRF1 co-localized with γ-tubulin, a microtubule and centrosomal marker, at the spindle poles and centrosomes (Figure 2E). In immunocytochemistry experiments aimed to determine the cellular localization pattern of the ZGRF1 variant proteins (Figure 2F), the wild-type ZGRF1 localized in a heterogeneous manner- majorly in the nucleus, occasionally in the cytoplasm, or both in the nucleus and cytoplasm, in HEK293 cells transiently overexpressing the ZGRF1 protein. The ZGRF1 variant proteins localized in a similar manner as the wild-type, with no apparent

disturbances in the localization patterns, or cellular morphological features. We estimated the steady state protein expression levels in whole cell lysates for the wild-type and variant proteins (Figure 2G). While ZGRF1 could be detected at the endogenous level in untransfected HEK293 cells, the steady state protein level was high in cells transfected with the *ZGRF1* wild-type allele. The six ZGRF1 variant proteins showed no difference in the expression levels as compared to the wild-type protein.

ZGRF1 variants and mitotic defects

We observed that the synchronized cultured cells expressing ZGRF1 variant proteins exhibited significant mitotic defects when compared to those expressing the ZGRF1 wild-type. These defects include multipolar cells with increased number of centrosomes, disoriented spindle poles or abnormal cytokinesis (Figure 3A). The highest extent of defects (Figure 3B) were observed for Thr602Ile (73.96%), Asp1984Gly (70.8%) and Phe1940Leu (69.32%). Comparable levels of defects were observed for the other variants, Glu660Gly (64.66%), R1862* (61%) and Arg326Gln (60.33%). We observed mitotic defects in cells overexpressing the wild-type protein (30.66%) as compared to its endogenous expression in untransfected cells. This suggests the need for optimal expression levels of ZGRF1 for cell division. The proportion of microtubule-based defects observed was however, significantly higher in cells expressing the ZGRF1 variant proteins (Figure 3C, Supplementary Figure S10). Mitotic defects in cells expressing ZGRF1 variant proteins during cell division and endogenous localization of the protein across mitotic stages, suggest its role in cell division.

ZGRF1 and UPF1 co-localize

In search for potential homologs for ZGRF1 by *in-silico* analysis, we found that the C-terminal region of ZGRF1 shows similarities with the helicase/ P-loop NTPase domain of DNA/RNA helicases bearing different types of zinc fingers. We obtained thirteen candidates with high significance values and from the highest similarity scores, we found UPF1 (Up-frameshift 1) to be the nearest paralog of ZGRF1 (Figure 4A, Supplementary Figure S11a). We then undertook pairwise alignment of ZGRF1 to the Protein Data Bank (PDB) UPF1-RNA complex (sequence ID: 2XZL, Chakrabarti et al 2011), which shows 29% identity and 46% similarity among the two proteins (Supplementary Figure S11b). UPF1 is a DNA/RNA helicase and a core protein of the nonsense-mediated mRNA decay (NMD) pathway. It is also involved in DNA repair, cell cycle regulation and genome stability. ZGRF1 and UPF1 have similar protein domains at their C-terminal region. Both proteins contain the DNA2 and

recD domains, have zinc fingers and helicase regions comprised of P-loop NTPase domain. UPF1 has been reported to be a cytoplasmic protein (Applequist et al 1997). We observed that ZGRF1 and UPF1 are present in the cell cytoplasm, and localize together at the centrosomes, nucleolus, and spindle poles during mitosis (Figure 4B). In dividing cells, we found UPF1 to co-localize with γ-tubulin at the spindle poles and spindle fibres (Supplementary Figure S11c).

Partial disruption of UPF1 localization in cells expressing ZGRF1 variants

HEK293 cells transfected with the ZGRF1-wildtype and ZGRF1-variants were co-stained for ZGRF1 and UPF1. Considering these two proteins co-localize in cellular compartments and at spindle poles during mitotic stages, it was of interest to examine impact, if any, on the UPF1 staining at spindles in the background of ZGRF1 wild-type and variant proteins. In this experiment, only cells with two spindle poles have been shown to maintain consistency in the data representation (n=60). Thr602Ile and Asp1984Gly showed substantial disruption in the UPF1 staining at the poles and microtubules (Figure 4C). For Arg1862* and Phe1940Leu milder disruption was observed in the overall staining for UPF1 in the poles and spindles. However, Arg326Gln and Glu660Gly did not influence the localization pattern of UPF1. Taken together, these observations suggest that ZGRF1 associates with UPF1 and that Thr602Ile and Asp1984Gly negatively influence the localization of UPF1 in a dividing cell.

Discussion

Variants in the *ZGRF1* gene were identified in this study of patients affected with hot water epilepsy (HWE). Though rare in their occurrence, cases of HWE have been reported from several parts of the world. Genetic causes underlying sensory reflex epilepsies are difficult to identify due to complex inheritance, clinical, genetic, etiological heterogeneity and gene-environment interactions (Italiano et al., 2016). However, during these recent years there has been progress to identify eight genes/ loci for light and sound induced epilepsies (Galizia et al., 2015; Kasteleijn-Nolst Trenite et al., 2015; Okudan and Özkara 2018).

HWE is triggered by the sensory stimuli of touch and temperature. While the cellular mechanisms underlying its manifestation are yet to be understood, cortical networks in predisposed individuals have been indicated to play a role (Ferlazzo et al., 2005). Certain genetic mutations that alter the somatosensory networks could render it susceptible to epileptic activity, upon exposure to specific stimuli. Mutations in genes identified for hot

water epilepsy include: *SYN1*, involved in neurotransmitter release and synaptogenesis identified in a French Canadian family (Fassio et al., 2011; Nguyen et al., 2015), *GPR56*, a regulator of neural precursor cell migration identified in a Portuguese boy (Öncü-Öner et al., 2018; Silva et al., 2015) and *SLC1A1* that alters glutamate transport and predispose to HWE was identified in Indian families (Karan et al., 2017).

We found six variants in ZGRF1 (p.Arg326Gln, p.Thr602Ile, p.Glu660Gly, p.Arg1862*, p.Phe1940Leu and p.Asp1984Gly) in HWE patients, including one (p.Thr602Ile) in the family (Family 227) where the locus was previously mapped (*HWE2*; Ratnapriya et al., 2009b). *HWE2* is one among the four known loci for HWE, three others being 10q21-q22 (*HWE1*, MIM: 613339, Ratnapriya et al., 2009a), 9p23-p24 (Karan et al., 2018) and 8p12-p23 (Karan et al., unpublished). *ZGRF1* is a mostly unexamined gene and therefore, we gathered clues about its potential cellular roles from a limited amount of literature and *in-silico* analysis. Potential variants in this gene have been found in other neurological and psychiatric disorders: p.Leu48Met and p.Glu1363Lys were reported in a multi-generation family with childhood apraxia of speech (Peter et al., 2016). p.Met502Val was identified in a large-scale exome study of schizophrenic individuals (Need et al., 2012).

In-silico analysis of ZGRF1 has suggested three major domains in the protein: DUF2439, zf-GRF and helicase. DUF2439 has been implicated in meiotic chromosome segregation, crossover recombination and telomere maintenance in yeast (Polakova et al., 2016; Silva et al., 2016). There are at least six other zinc fingers GRF-type proteins involved in aspects of DNA damage response, transcription or RNA regulatory activities. We found the helicase domain of ZGRF1 to be homologous to DNA/RNA helicases, with UPF1 (Up-frameshift 1) being its nearest paralog. UPF1 is a core protein of the nonsense-mediated mRNA decay (NMD) pathway which is expressed at high levels in the hippocampus of patients with intractable temporal lobe epilepsy and mice, post status epilepticus (Mooney et al., 2017). We observed ZGRF1 and UPF1 to localize in the nucleolus, centrosomes and spindle poles in cultured mammalian cells. Interestingly, UPF1 localization at the spindles is substantially affected by p.Thr602Ile and p.Asp1984Gly, and partially, by p.Arg1862* and p.Phe1940Leu. This suggests that the two proteins interact, and ZGRF1 plays molecular roles similar to that of UPF1. ZGRF1 also belongs to the family of UPF1-like RNA helicases that are involved in aspects of DNA replication and repair, transcription regulation, RNA metabolism, genome integrity or topoisomerase activities. Mutations in genes belonging to this family have been

implicated in neurological conditions like distal spinal muscular atrophy (*IGHMBP2*, Grohmann et al., 2001) and spinocerebellar ataxia and amyotrophic lateral sclerosis (*SETX*, Fogel et al., 2014).

Cellular localization studies show ZGRF1 to be prominently present at the centrosomes. Further, it was seen to localize with γ-tubulin at the spindle poles indicating a role of this protein in cell cycle. ZGRF1 variants lead to varying degrees of microtubule-based defects in the form of multipolar cells, disoriented spindles, misaligned chromosomes and abnormal cytokinesis, during mitosis. The variants p.Thr602Ile, Phe1940Leu and p.Asp1984Gly caused significant (2.2-2.4 folds) mitotic defects as compared to the wild-type protein. The other three variants Arg326Gln, Glu660Gly and Arg1862* caused 1.9-2 folds such defects. Interestingly, overexpression of the wild-type protein results in certain level of defects and incorporation of the variant proteins exacerbates this during mitosis. It is of interest to notice that centrosomal and cell cycle proteins like *CDKL5* (Barbiero et al., 2017) and *EFHC1* (de Nijs et al., 2012) have been previously reported for human epilepsy syndromes. *ZGRF1* variants identified in this study provide genetic evidences and preliminary insights into unanticipated roles of this novel protein underlying HWE. Functional consequences of the *ZGRF1* variants in cell-based assays indicate that subtle cellular defects in physiological conditions may contribute to pathophysiology of this disorder.

At least two earlier reports identified *ZGRF1* as a candidate for DNA crosslink resistance (Smogorzewska et al., 2010), and regulator of mammalian homologous recombination (HR) machinery (Adamson et al., 2012). Our observations (data not presented here) suggest cytoplasm-nucleus shuttling activity of ZGRF1 in response to DNA damage and repair response, and localization at the processing bodies hinting a role in mRNA surveillance and decay (Parker and Sheth, 2007). Genes underlying sensory epilepsies encompass channel proteins, neurotransmitter regulators, receptors and DNA helicases, and ZGRF1 is an interesting candidate addition to this diversity of molecules. ZGRF1 is a multi-domain and multi-functional protein. Better understanding of its molecular roles could be achieved by studies in cultured mammalian cells incorporated with the HWE variants and domain-specific mutants created by CRISPR/Cas9 method. We propose that further studies involving *ZGRF1*$^{-/-}$ null mice could provide insights into the mechanistic basis of *ZGRF1* in hot water epilepsy. Studies involving ZGRF1 expression patterns in the wild-type and null mouse brain, examining dendritic arborisation in hippocampus and cortex in vivo and in primary

cultures would shed light into the role of this protein. It would be interesting to induce seizures in these mice with hot water jets and examine for neuronal sprouting, as previously described as a phenomenon of hyperthermic seizures (Ullal et al., 1996; Ullal et al., 2006). ChIP-sequencing in wild-type mice and transcriptome analysis of the *ZGRF1*$^{-/-}$ null and wild-type mice brains would provide insights into the genetic networks of *ZGRF1*, and allow further understanding the functions of this protein, its role in the brain and in hot water epilepsy.

Web resources

The URLs for the web resources used in this study are:
RefSeq (https://www.ncbi.nlm.nih.gov/refseq/), Primer3 (http://bioinfo.ut.ee/primer3-0.4.0/), NCBI HomoloGene database (https://www.ncbi.nlm.nih.gov/homologene/), Clustal Omega (https://www.ebi.ac.uk/Tools/msa/clustalo//), SIFT (https://sift.bii.a-star.edu.sg/), PolyPhen-2 (http://genetics.bwh.harvard.edu/pph2/), Mutation Taster (http://www.mutationtaster.org/), and FATHMM (http://fathmm.biocompute.org.uk/). DELTA-BLAST and pBLAST (https://blast.ncbi.nlm.nih.gov/Blast.cgi?PROGRAM=blastp&PAGE_TYPE=BlastSearch&LINK_LOC=blasthome), EMBOSS Needle (https://www.ebi.ac.uk/Tools/psa/emboss_needle/),1000 Genomes (https://www.internationalgenome.org/1000-genomes-browsers/), Ensembl (https://asia.ensembl.org/index.html), Exome Sequencing Project (ESP) (https://evs.gs.washington.edu/EVS/), gnomAD (https://gnomad.broadinstitute.org/), NCBI Variation Viewer (https://www.ncbi.nlm.nih.gov/variation/view/).

Acknowledgements The authors thank the individuals with hot water epilepsy and their families for participation in this study. We thank Sambhavi Puri for her inputs and validation of the mitotic defects experiments; and RamShankar Mani, Nishtha Pandey, Praveen Raju and Kalpita Karan for their comments on the manuscript. This work is supported by funds from ICMR, New Delhi; DBT, New Delhi and JNCASR, Bangalore. SRC acknowledges receipt of research fellowship from CSIR, New Delhi.

Conflict of interest All authors report no financial interests or potential conflicts of interests.

References

Adamson B, Smogorzewska A, Sigoillot FD, King RW, Elledge SJ (2012) A genome-wide homologous recombination screen identifies the RNA-binding protein RBMX as a component of the DNA-damage response. Nat Cell Biol 14:318–328

Adzhubei IA, Schmidt S, Peshkin L, Ramensky VE, Gerasimova A, Bork P, Kondrashov AS, Sunyaev SR (2010) A method and server for predicting damaging missense mutations. Nat Methods 7:248–249

Allen IM (1945) Observations on cases of reflex epilepsy. New Zealand Med. J. 44:135-142

Barbiero I, Valente D, Chandola C, Magi F, Bergo A, Monteonofrio L, Tramarin M, Fazzari M, Soddu S, Landsberger N, Rinaldo C, Kilstrup-nielsen C (2017) CDKL5 localizes at the centrosome and midbody and is required for faithful cell division. Sci Rep 7:1–12

Bebek N, Gürses C, Gokyigit A, Baykan B, Ozkara C, Dervent A (2001) Hot water epilepsy: Clinical and electrophysiologic findings based on 21 cases. Epilepsia 42:1180–1184

Boratyn GM, Schäffer AA, Agarwala R, Altschul SF, Lipman DJ, Madden TL (2012) Domain enhanced lookup time accelerated BLAST. Biol Direct 7:12

Cheng Z, Muhlrad D, Lim MK, Parker R, Song H (2007) Structural and functional insights into the human Upf1 helicase core. EMBO J 26:253–64

de Nijs L, Wolkoff N, Coumans B, Delgado-escueta AV, Grisar T, Lakaye B (2012) Mutations of EFHC1 , linked to juvenile myoclonic epilepsy, disrupt radial and tangential migrations during brain development. Human Mol Genet 21:5106–5117

Engel J, International League Against Epilepsy (ILAE) (2001) A proposed diagnostic scheme for people with epileptic seizures and with epilepsy: report of the ILAE Task Force on Classification and Terminology. Epilepsia 42:796–803

Fassio A, Patry L, Congia S, Onofri F, Piton A, Gauthier J, Pozzi D, Messa M, Defranchi E, Fadda M, Corradi A, Baldelli P, Lapointe L, St-Onge J, Meloche C, Mottron L, Valtorta F, Nguyen DK, Rouleau GA, et al (2011) SYN1 loss-of-function mutations in autism and partial epilepsy cause impaired synaptic function. Hum Mol Genet 20:2297–2307

Ferlazzo E, Zifkin BG, Andermann E, Andermann F (2005) Cortical triggers in generalized reflex seizures and epilepsies. Brain 128:700–710

Fogel BL, Cho E, Wahnich A, Gao F, Becherel OJ, Wang X, Fike F, Chen L, Criscuolo C, Michele G De, Filla A, Collins A, Hahn AF, Gatti RA, Konopka G, Perlman S, Lavin MF, Geschwind DH, Coppola G (2014) Mutation of senataxin alters disease-specific transcriptional networks in patients with ataxia with oculomotor apraxia type 2. Hum Mol Genet 23:4758–4769

Frickey T, Lupas AN (2004) Phylogenetic analysis of AAA proteins. J Struct Biol 146:2–10

Galizia EC, Myers ÃCT, Leu ÃC, Kovel ÃCGF De, Afrikanova T, Cordero-maldonado ML, Martins TG, Jacmin M, Drury S, Chinthapalli VK, Muhle H, Pendziwiat M, Sander T, Ruppert A, Møller RS, Thiele H, Krause R, Schubert J, Lehesjoki A, et al (2015) CHD2 variants are a risk factor for photosensitivity in epilepsy. Brain 138:1198–1207

Grohmann K, Schuelke M, Diers A, Hoffmann K, Lucke B, Adams C, Bertini E, Leonhardt-horti H, Muntoni F, Ouvrier R, Pfeufer A, Maldergem L Van, Wilmshurst JM, Wienker TF, Sendtner M (2001) Mutations in the gene encoding immunoglobulin µ - binding protein 2 cause spinal muscular atrophy with respiratory distress type 1. Nat Genet 29:75–77

Italiano D, Striano P, Russo E, Leo A, Spina E, Zara F, Striano S, Gambardella A, Labate A, Gasparini S, Lamberti M, De Sarro G, Aguglia U, Ferlazzo E (2016) Genetics of reflex seizures and epilepsies in humans and animals. Epilepsy Res 121:47–54

Iyer LM, Leipe DD, Koonin E V, Aravind L (2004) Evolutionary history and higher order classification of AAA+ ATPases. J Struct Biol 146:11–31

Karan KR, Satishchandra P, Sinha S (2018) A genetic locus for sensory epilepsy precipitated by contact with hot water maps to chromosome 9p24.3-p23. J Genet 97:391–398

Karan KR, Satishchandra P, Sinha S, Anand A (2017) Rare *SLC1A1* variants in hot water epilepsy. Hum Genet 136:693–703

Kasteleijn-Nolst Trenite DGA, Volkers L, Strengman E, Schippers HM, Perquin W, Haan G De, Gkountidi AO, Van R, Graaf SF Van De, Jocic-jakubi B, Capovilla G, Covanis A, Parisi P, Veggiotti P, Brinciotti M, Incorpora G, Piccioli M, Cantonetti L, Berkovic SF, Scheffer IE, et al (2015) Clinical and genetic analysis of a family with two rare reflex epilepsies. Seizure 29:90–96

Keipert JA (1969) Epilepsy precipitated by bathing: water-immersion epilepsy. J Paediatr Child Health 5:244–247

Kumar P, Henikoff S, Ng PC (2009) Predicting the effects of coding non-synonymous variants on protein function using the SIFT algorithm. Nat Protoc 4:1073–1081

Kurata S (1979) Epilepsy precipitated by bathing-A follow-up study. Brain Dev (Domestic ed) 11:400–405

Li H, Durbin R (2009) Fast and accurate short read alignment with Burrows-Wheeler transform. Bioinformatics 25:1754–1760

Li H, Handsaker B, Wysoker A, Fennell T, Ruan J, Homer N, Marth G, Abecasis G, Durbin R, 1000 Genome Project Data Processing Subgroup 1000 Genome Project Data Processing (2009) The Sequence Alignment/Map format and SAMtools. Bioinformatics 25:2078–9

Mani KS, Mani AJ, Ramesh CK (1974) Hot-water epilepsy-a peculiar type of reflex epilepsy: clinical and EEG features in 108 cases. Trans Am Neurol Assoc 99:224–226

Mooney CM, Jimenez-Mateos EM, Engel T, Mooney C, Diviney M, Venø MT, Kjems J, Farrell MA, O'Brien DF, Delanty N, Henshall DC (2017) RNA sequencing of synaptic and cytoplasmic Upf1-bound transcripts supports contribution of nonsense-mediated decay to epileptogenesis. Sci Rep 7:41517

Moran J (1976) So-called water immersion epilepsy. Ir J Med Sci 145:140

Morimoto T, Hayakawa T, Sugie H, Awaya Y, Fukuyama Y (1985) Epileptic Seizures Precipitated by Constant Light, Movement in Daily Life, and Hot Water Immersion. Epilepsia 26:237–242

Need AC, McEvoy JP, Gennarelli M, Heinzen EL, Ge D, Maia JM, Shianna KV, He M, Cirulli ET, Gumbs CE, Zhao Q, Campbell CR, Hong L, Rosenquist P, Putkonen A, Hallikainen T, Repo-Tiihonen E, Tiihonen J, Levy DL, et al (2012) Exome Sequencing Followed by Large-Scale Genotyping Suggests a Limited Role for Moderately Rare Risk Factors of Strong Effect in Schizophrenia. Am J Hum Genet 91:303–312

Nguyen DK, Rouleau I, Sénéchal G, Ansaldo AI, Gravel M, Benfenati F, Cossette P (2015) X-linked focal epilepsy with reflex bathing seizures: Characterization of a distinct epileptic syndrome. Epilepsia 56:1098–1108

Okudan ZV, Özkara Ç (2018) Reflex epilepsy: triggers and management strategies. Neuropsychiatr Dis Treat. 14: 327–337

Öncü-Öner T, Ünalp A, Porsuk-doru İ, Ağılkaya S (2018) GPR56 homozygous nonsense mutation p.R271* associated with phenotypic variability in bilateral frontoparietal polymicrogyria. Turkish J Pediatr 56:229–237

Parker R, Sheth U (2007) P Bodies and the Control of mRNA Translation and Degradation. Mol Cell 25:635–646

Peter B, Wijsman EM, Nato AQ, Matsushita MM, Chapman KL, Stanaway IB, Wolff J, Oda K, Gabo VB, Raskind WH, Raskind WH (2016) Genetic Candidate Variants in Two Multigenerational Families with Childhood Apraxia of Speech. PLoS One 11:e0153864

Polakova S, Molnarova L, Hyppa RW, Benko Z, Misova I, Schleiffer A, Smith GR, Gregan J (2016) Dbl2 Regulates Rad51 and DNA Joint Molecule Metabolism to Ensure Proper Meiotic Chromosome Segregation. PLoS Genet 12:e1006102

Quinlan AR, Hall IM (2010) BEDTools: a flexible suite of utilities for comparing genomic features. Bioinformatics 26:841–842

Raney KD, Byrd AK, Aarattuthodiyil S (2013) Structure and Mechanisms of SF1 DNA Helicases. Adv Exp Med Biol 767:1-32

Ratnapriya R, Satishchandra P, Kumar SD, Gadre G, Reddy R, Anand A (2009a) A locus for autosomal dominant reflex epilepsy precipitated by hot water maps at chromosome 10q21.3-q22.3. Hum Genet 125:541–549

Ratnapriya R, Satishchandra P, Dilip S, Gadre G, Anand A (2009b) Familial autosomal dominant refex epilepsy triggered by hot water maps to 4q24-q28. Hum Genet 126:677–683

Santos-Silva R, Passas A, Rocha C, Figueiredo R, Mendes-Ribeiro J, Fernandes S, Biskup S, Leão M (2015) Bilateral frontoparietal polymicrogyria: A novel GPR56 mutation and an unusual phenotype. Neuropediatrics 46:134–138

Satishchandra P (2003) Geographically Specific Epilepsy Syndromes in India Hot-Water Epilepsy. Epilepsia 44:29–32

Satishchandra P, Shivaramakrishana A, Kaliaperumal VG, Schoenberg BS (1988) Hot-Water Epilepsy: A Variant of Reflex Epilepsy in Southern India. Epilepsia 29:52–56

Schwarz JM, Rödelsperger C, Schuelke M, Seelow D (2010) MutationTaster evaluates disease-causing potential of sequence alterations. Nat Methods 7:575–576

Shihab HA, Gough J, Cooper DN, Stenson PD, Barker GLA, Edwards KJ, Day INM, Gaunt TR (2013) Predicting the Functional, Molecular, and Phenotypic Consequences of Amino Acid Substitutions using Hidden Markov Models. Hum Mutat 34:57–65

Silva S, Altmannova V, Luke-Glaser S, Henriksen P, Gallina I, Yang X, Choudhary C, Luke B, Krejci L, Lisby M (2016) Mte1 interacts with Mph1 and promotes crossover recombination and telomere maintenance. Genes Dev 30:700–717

Smogorzewska A, Desetty R, Saito TT, Schlabach M, Lach FP, Sowa ME, Clark AB, Kunkel TA, Harper JW, Colaiácovo MP, Elledge SJ (2010) A Genetic Screen Identifies FAN1, a Fanconi Anemia-Associated Nuclease Necessary for DNA Interstrand Crosslink Repair. Mol Cell 39:36–47

Stensman R, Ursing B (1971) Epilepsy precipitated by hot water immersion. Neurology 21:559–562

Szymonowicz W, Meloff KL (1978) Hot Water Epilepsy. Can J Neurol Sci 5:247–251

Ullal GR, Satishchandra P, Kalladka D, Rajashekar K, Archana K, Mahadevan A, Shankar SK (2006) Kindling & mossy fibre sprouting in the rat hippocampus following hot water induced hyperthermic seizures. Indian J Med Res 124:331–342

Ullal GR, Satishchandra P, Shankar SK (1996) Hyperthermic seizures: an animal model for hot-water epilepsy. Seizure 5:221–228

Table 1: *ZGRF1* variants among HWE patients

Nucleotide change	Amino acid change	rsID	Occurrence in patients (n=288)	MAF in control individuals (n=288)	MAF in dbSNP 144, 1000G, ESP, or ExAC	Conservation Score[a]	SIFT Score[b]	PolyPhen-2 Hum Var Score[c]	Mutation Taster Probability Value[d]	FATHMM Score[e]
c.977G>A	p.Arg326Gln	rs535674967	1	0	0.0002 (dbSNP), 0.0002 (1000G), 0.00004 (gnomAD)	0.015	Tolerated 0.26	Probably damaging 0.998	Polymorphism 0.923	Damaging -1.96
c.1805C>T	p.Thr602Ile	rs201904239	3	0.0034	0.0012 (dbSNP), 0.001 (1000G), 0.0008 (gnomAD)	0.601	Damaging 0.03	Benign 0.012	Polymorphism 0.999	Damaging -1.64
c.1979A>G	p.Glu660Gly	-	1	0	-	-0.817	Damaging 0.05	Benign 0.013	Polymorphism 0.999	Damaging -2.02
c.5584C>T	p.Arg1862*	rs767296222	2	0	0.00004 (gnomAD)	-1.202	Damaging 0.01	-	Disease causing 0.999	-
c.5818T>C	p.Phe1940Leu	rs773566516	2	0	0.00001 (gnomAD)	-1.094	Damaging0	Benign 0.284	Disease causing 0.967	Damaging -2.86
c.5951A>G	p.Asp1984Gly	rs780748235	1	0.0017	0.00004 (gnomAD)	1.562	Tolerated 0.35	Benign 0.108	Polymorphism 0.999	Tolerated -1.13

(RefSeq id: NM_018392.4, CCDS3700.2)

[a] The Consurf Server; conservation scores for the amino acids based on the phylogenetic relationship from 41 homologous sequences (Ashkenazy et al 2010).

[b] Sorting Intolerant From Tolerant [SIFT] (Kumar et al 2009) : SIFT predicts for amino acid substitutions with scores ranging from 0-1. Variant scores ranging from 0.0-0.05 are considered deleterious, with scores closer to 0.0 being confidently predictive of deleteriousness. Scores between 0.05-1.0 are considered tolerated, with scores closer to 1.0 suggest that the variant is tolerable.

[c] Polymorphism Phenotyping v2 [PolyPhen-2] (Adzhubei et al 2010) : PolyPhen predicts for amino acid substitutions with scores ranging from 0-1 as being benign to damaging.

[d] Mutation Taster (Schwarz et al 2010) : Probability of prediction; values close to 1 indicates a high security of the prediction.

[e] Functional Analysis through Hidden Markov Models (FATHMM) (Shihab et al 2013) : Combines sequence conservation with hidden Markov models to determine ‘pathogenecity weights’

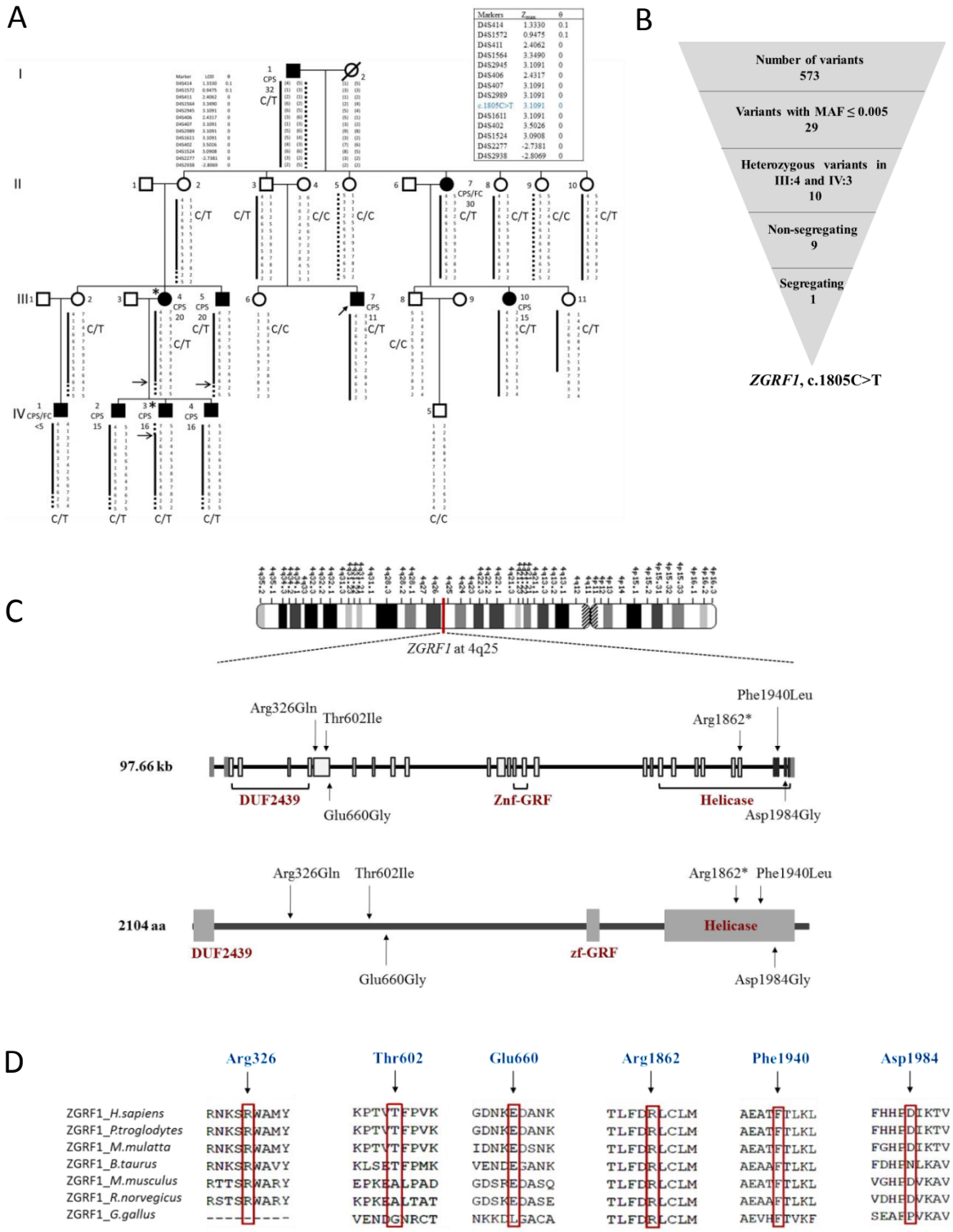

Figure 1: *ZGRF1* at 4q24-q28. (A) Pedigree of Family 227 showing the segregation of the disease haplotype and c.1805C>T. Individuals marked with an asterisk (*) were whole-exome sequenced (modified from Ratnapriya et al., 2009b). The maximum LOD score obtained for the markers and for the variant is represented in the box. (B) Work flow for screening and filtering the gene variants in the 4q24-q28 target region. (C) Chromosomal location, gene structure and protein structure of ZGRF1 showing the positions of the six rare variants. (D) Amino acid conservation of the six residues across certain species.

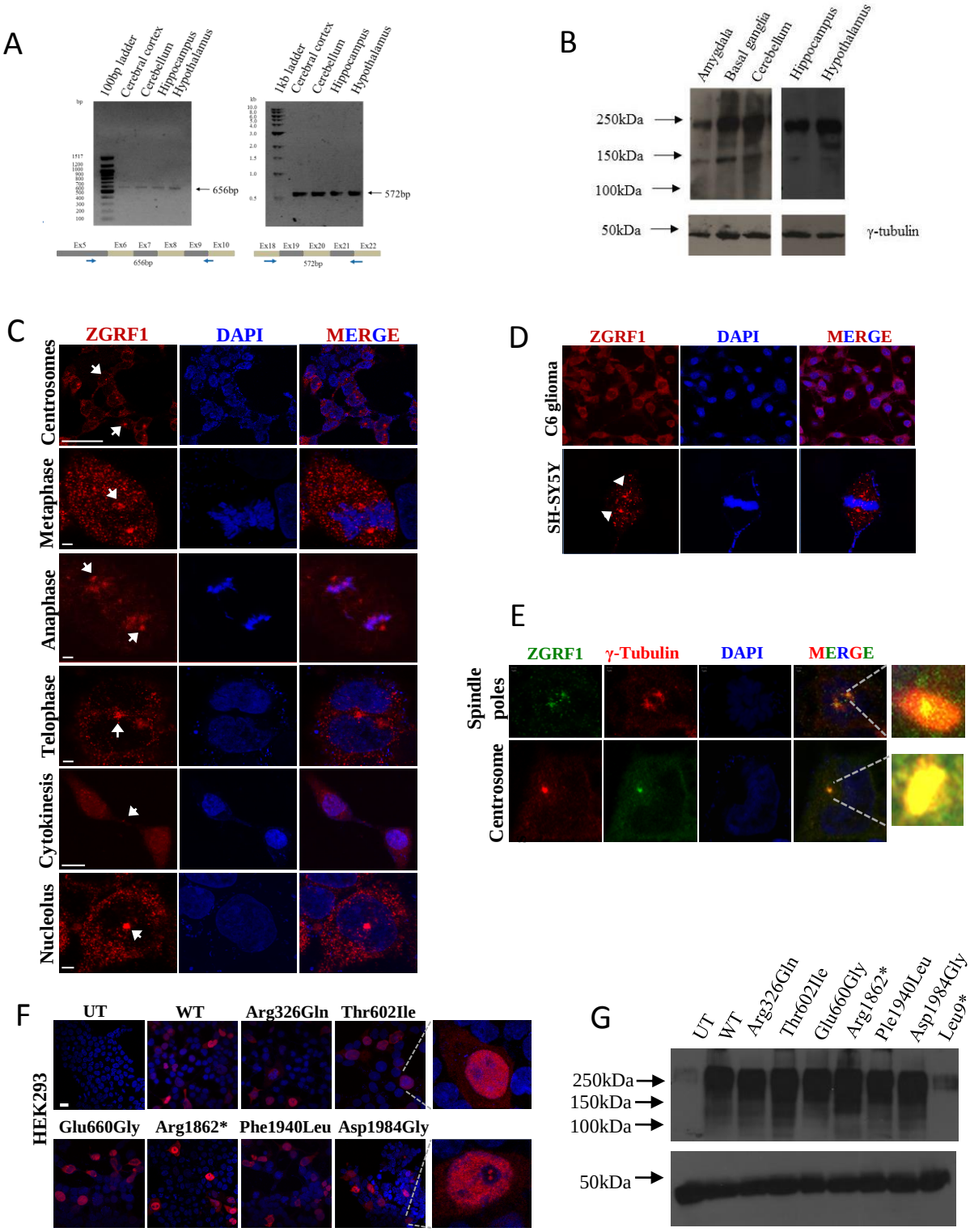

Figure 2: Expression of ZGRF1. (A) Expression of ZGRF1 transcripts in different regions of the human brain. (B) ZGRF1 protein expression in different human brain regions. (C) Endogenous localization of ZGRF1 in cultured HEK293 cells. Arrows indicate specific localizations of the protein. Scale bars = 20 µm, 5 µm. (D) Endogenous localization of ZGRF1 in C6 glioma and SH-SY5Y cells. Arrows point towards spindle poles. (E) Co-localization of ZGRF1 with γ-tubulin at spindle poles and centrosomes. (F) Localization of overexpressed ZGRF1- wild-type and mutant proteins in the nucleus of HEK293. Scale bar = 20 µm. (G) Untransfected and overexpressed ZGRF1 wild-type and variant proteins in HEK293.

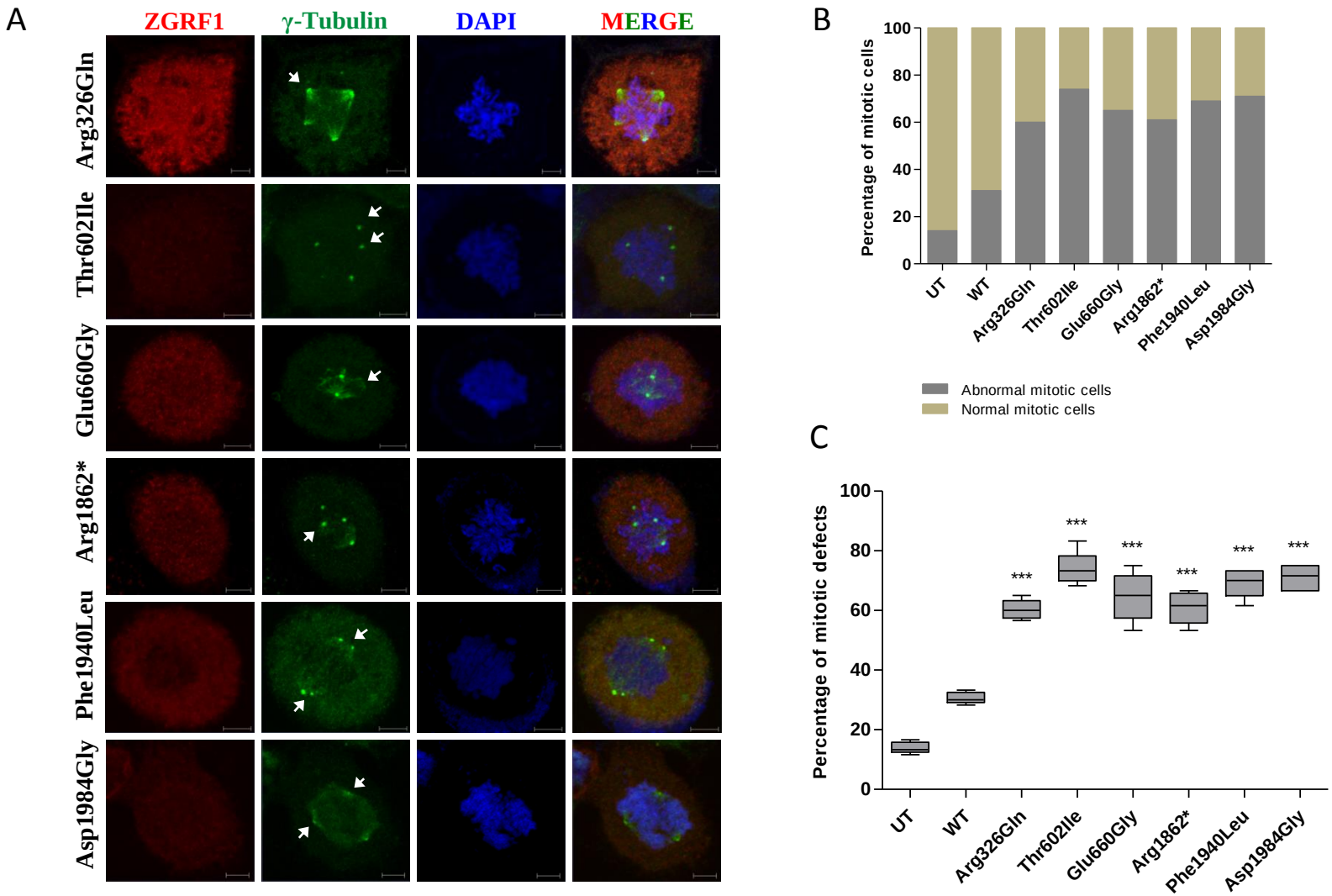

Figure 3: Mitotic defects in cells with ZGRF1 variants. (A) Defective cells with multipolar or disoriented spindles. Arrows indicate towards spindle poles. Scale bar = 5μm. (B) Percentage of normal and abnormal cells (with mitotic defects) in untransfected, wild-type and six ZGRF1 variants examined (n=300). (C) Statistical quantification of the percentage of abnormal mitotic cells in the untransfected, wild-type and six ZGRF1 variants (***$P \leq 0.001$).

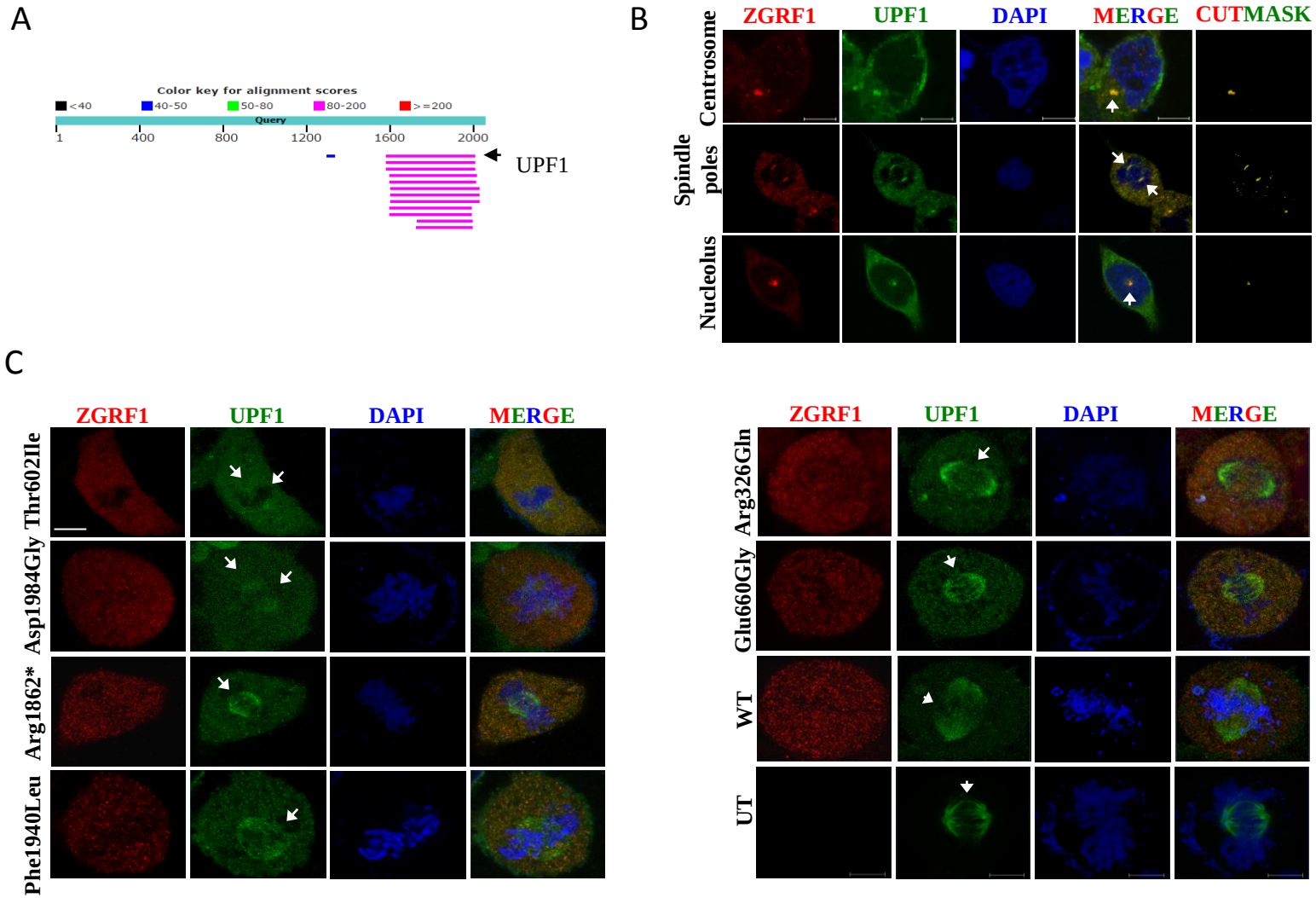

Figure 4: Expression analysis of ZGRF1 and UPF1. (A) BLAST alignment output for the ZGRF1 full-length protein. (B) ZGRF1 and UPF1 in cultured HEK293 cells co-localize in the centrosomes, spindle poles and nucleolus indicated by arrows. Cutmask represents the regions of co-localization. Scale bar = 5 µm. (C) UPF1 localization to spindles was substantially disrupted by the Thr602Ile and Asp1984Gly variants, partially disrupted by Arg1862* and Phe1940Leu and unaffected by Arg326Glu and Glu660Gly. Arrows point towards spindle poles and microtubules. Scale bar = 5 µm.